Science Signaling
AAAS

stke.sciencemag.org/cgi/content/full/12/592/eaav5637/DC1

Supplementary Materials for

Noncompetitive inhibitors of TNFR1 probe conformational activation states

Chih Hung Lo, Tory M. Schaaf, Benjamin D. Grant, Colin Kin-Wye Lim, Prachi Bawaskar, Courtney C. Aldrich, David D. Thomas, Jonathan N. Sachs*

*Corresponding author. Email: jnsachs@umn.edu

Published 30 July 2019, *Sci. Signal.* **12**, eaav5637 (2019)
DOI: 10.1126/scisignal.aav5637

This PDF file includes:

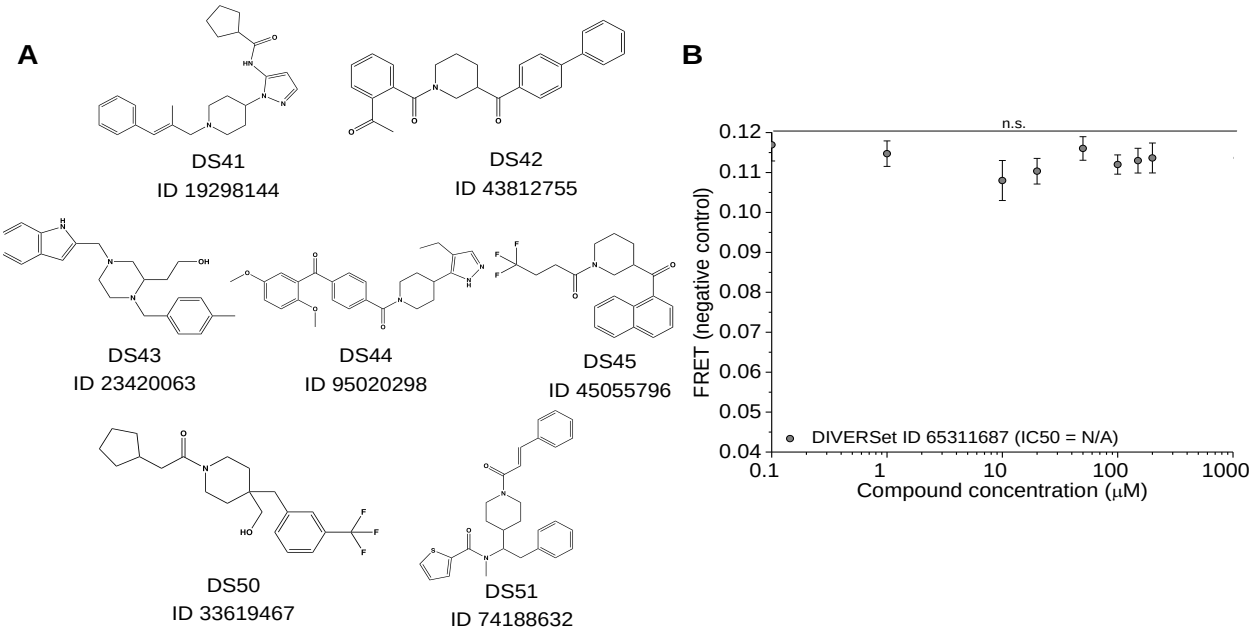

Fig. S1. Chemical structures of the novel small molecule inhibitors of TNFR1 and a negative control compound. (**A**) The chemical structures and the ChemBridge IDs of the seven previously unidentified small molecules, discovered from high-throughput screening of the ChemBridge DIVERSet 50,000 compound library, that perturb the conformational states of the pre-assembled TNFR1 dimer. (**B**) No FRET change was observed with a negative control compound. Data are means ± SD of three independent experiments and n.s. indicates not significant by two-tailed unpaired *t* test.

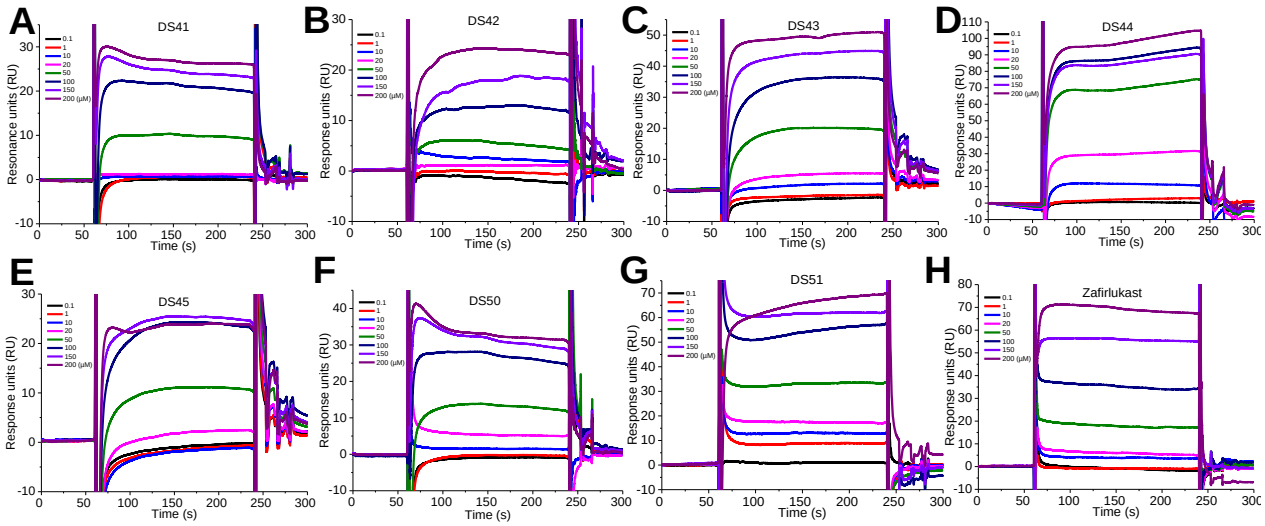

Fig. S2. The seven hit compounds and zafirlukast bind the TNFR1 ECD as characterized by SPR measurements. SPR raw binding curves for (**A**) DS41, (**B**) DS42, (**C**) DS43, (**D**) DS44, (**E**) DS45, (**F**) DS50, (**G**) DS51, and (**H**) zafirlukast. Bind curves are representative of three independent experiments.

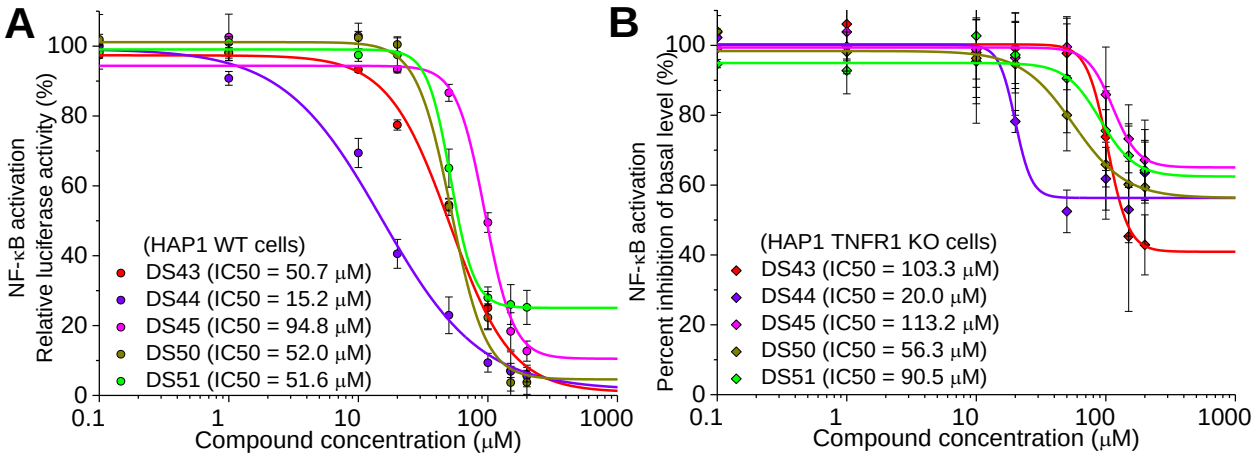

Fig. S3. Some hit compounds nonspecifically inhibit TNFR1-stimulated NF-κB activation. (**A** and **B**) NF-κB activation in WT HAP1 cells (A) and TNFR1 KO HAP1 cells (B) treated with LTα and increasing concentration of hit compounds (DS43, DS44, DS45, DS50 and DS51) to test the compound specificity to TNFR1. Data are means ± SD of three independent experiments.

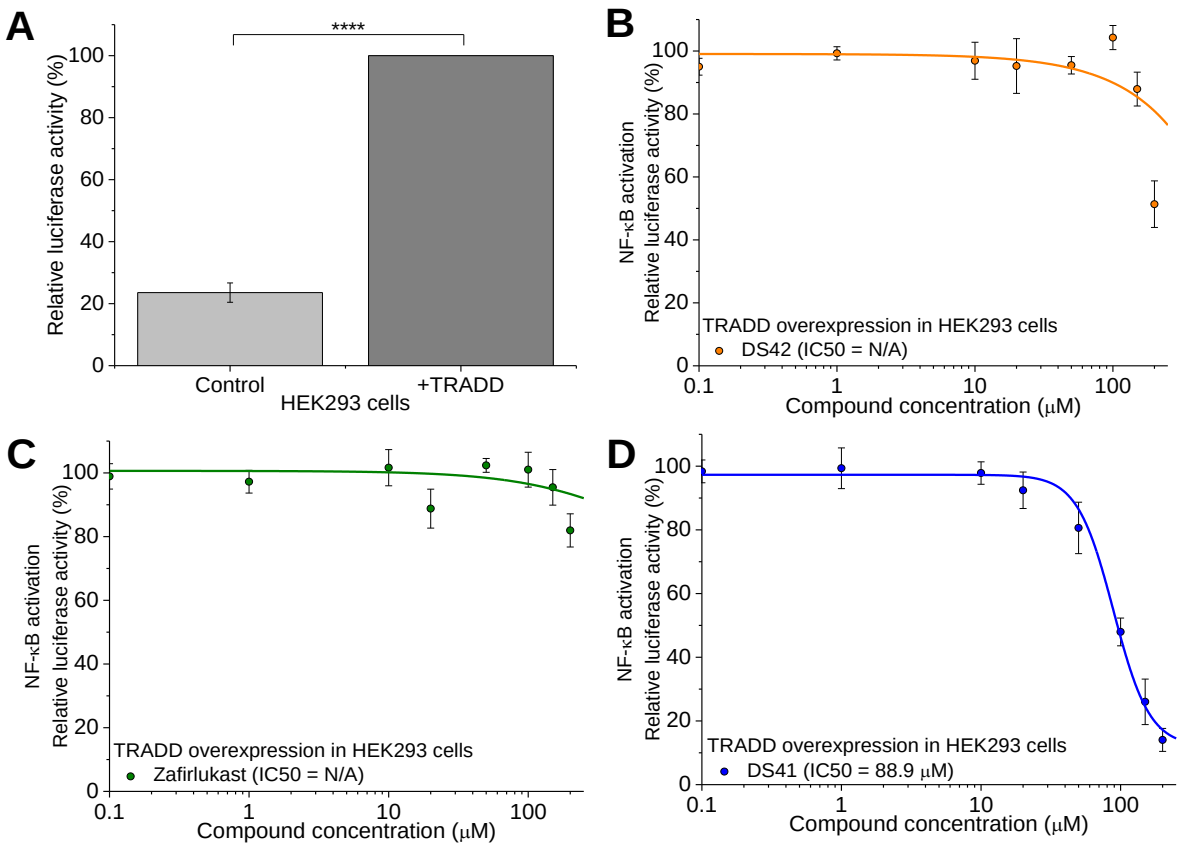

Fig. S4. DS41, but not DS42 and zafirlukast, inhibits TRADD-induced NF-κB activation in HEK293 cells. (**A**) NF-κB activation in HEK293 cells expressing reporter plasmids and control plasmids (no TRADD) or TRADD plasmids and treated with DMSO control. Data are means ± SD of three independent experiments and ****$P < 0.0001$ compared to control by two-tailed unpaired *t* test. (**B** to **D**) TRADD-induced NF-κB activation from (A) in HEK293 cells treated with increasing concentration of DS42 (B), zafirlukast (C) or DS41 (D). Data are means ± SD of three independent experiments.

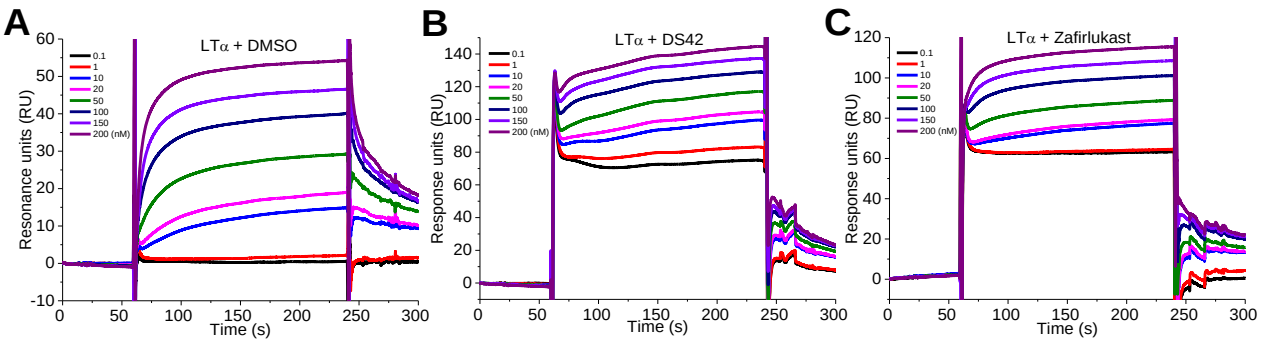

Fig. S5. Small-molecule inhibitors do not disrupt ligand-receptor interactions as characterized by SPR measurements. SPR raw binding curves for (**A**) LTα and DMSO, (**B**) LTα and DS42, and (**C**) LTα and zafirlukast. Binding curves are representative of three independent experiments.

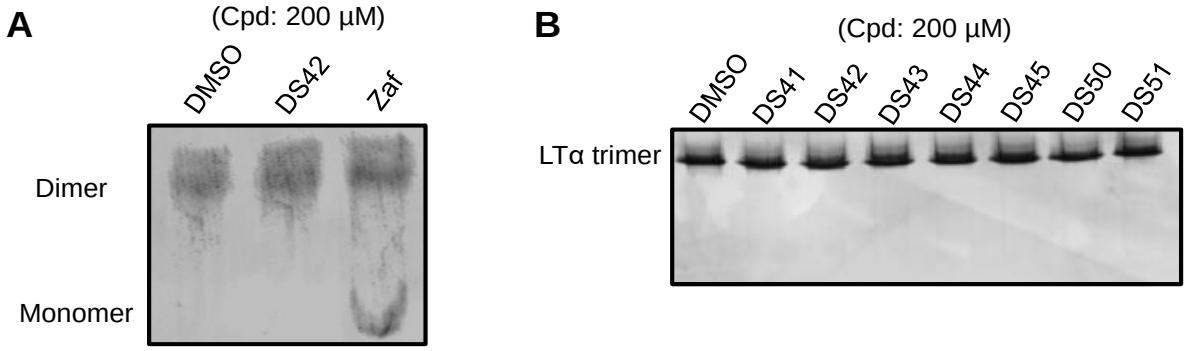

Fig. S6. Hit compounds do not disrupt either the TNFR1 PLAD dimer or the LTα trimer. (**A**) Western blot analysis of soluble TNFR1 PLAD with treatment of DMSO control, DS42 and zafirlukast. Western blots are representative of three independent experiments. (**B**) Native gel characterization of LTα with treatments of DMSO control and hit compounds. Gels are representative of three independent experiments.

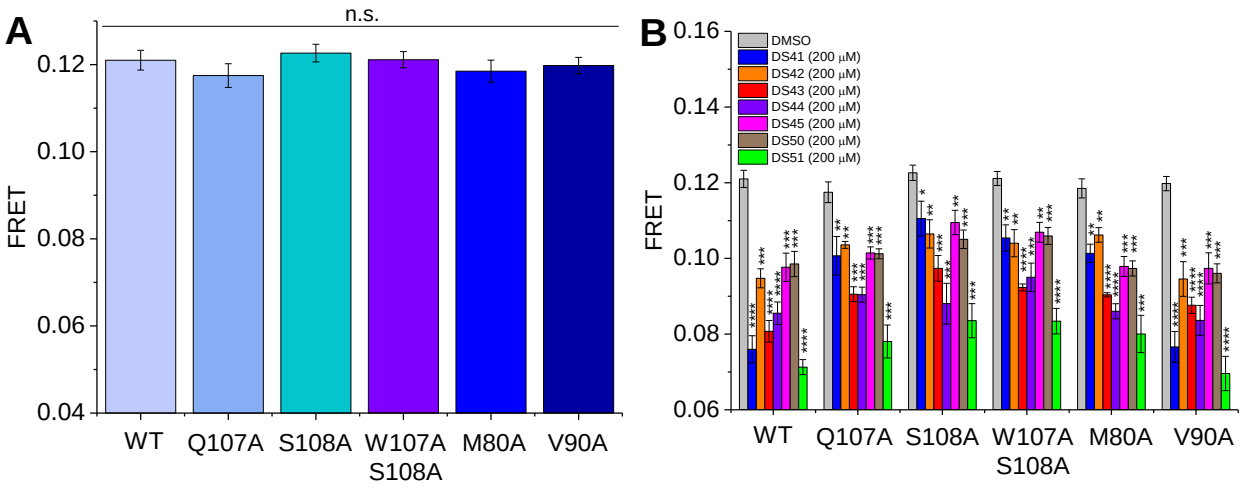

Fig. S7. Hit compounds reduce FRET mediated by the TNFR1 mutant biosensors. (**A**) TNFR1 FRET biosensors were created with mutations in the ligand binding loop and the conformationally active region of the receptor (W107A, S108A, WS107/108AA and M80A). A control FRET biosensor with a mutation (V90A) that is located far from the ligand binding loop was also created. Basal FRET was calculated for all the biosensors are shown. Data are means ± SD of three independent experiments and n.s. indicates not significant by two-tailed unpaired *t* test. (**B**) Analysis of the effect of the hit compounds (200 μM) on FRET mediated by the TNFR1 mutant biosensors. Data are means ± SD of three independent experiments and **P* < 0.05, ***P* < 0.01, ****P* < 0.001, *****P* < 0.0001 by two-tailed unpaired *t* test.

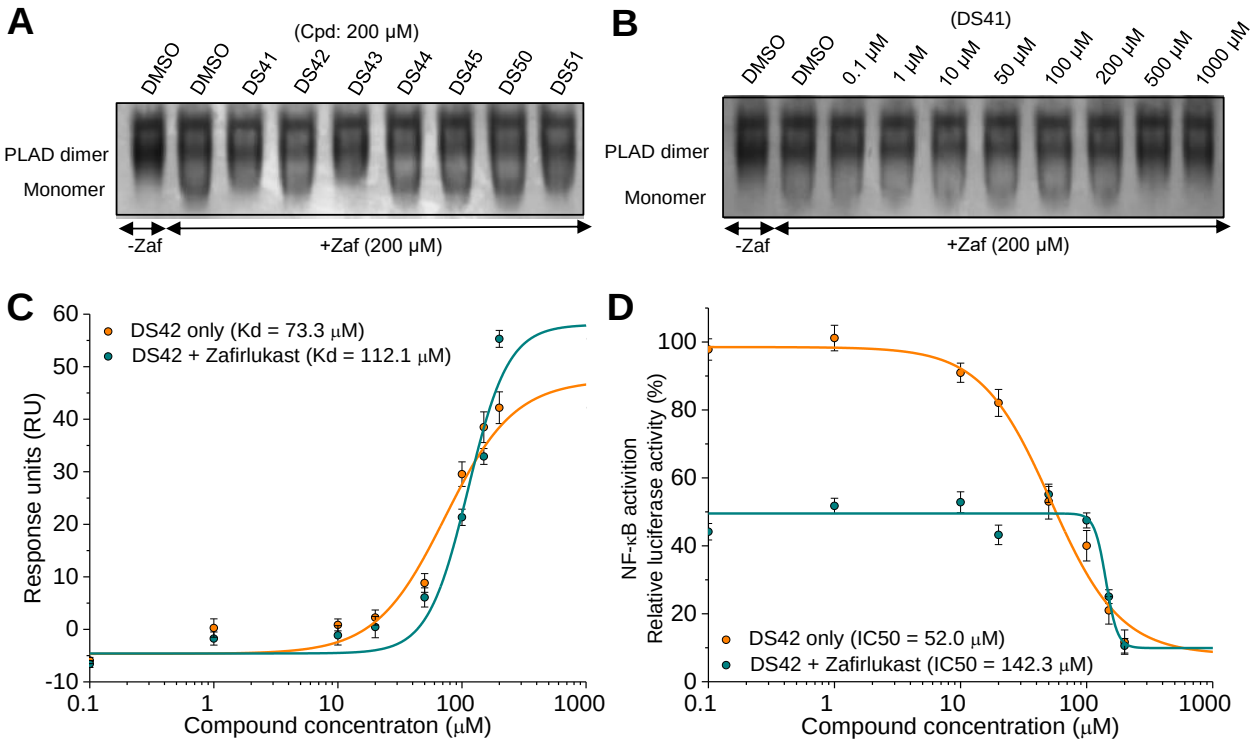

Fig. S8. Hit compounds compete with zafirlukast in binding to the TNFR1 PLAD and in inhibiting NF-κB activation. (**A**) Native gel characterization of soluble TNFR1 PLAD cotreated with the hit compounds (200 µM) and zafirlukast (200 µM). Gels are representative of three independent experiments. (**B**) Native gel characterizations of soluble TNFR1 PLAD from cells cotreated with increasing concentrations of DS41 (0.1 to 1000 µM) and a single dose of zafirlukast (200 µM). Gels are representative of three independent experiments. (**C**) SPR competition assay using increasing concentrations of DS42 and a single dose of zafirlukast (100 µM). Data are means ± SD of three independent experiments. (**D**) NF-κB activation in HEK293 cells treated with LTα, increasing concentration of DS42 and a single dose of zafirlukast (100 µM). Data are means ± SD of three independent experiments.

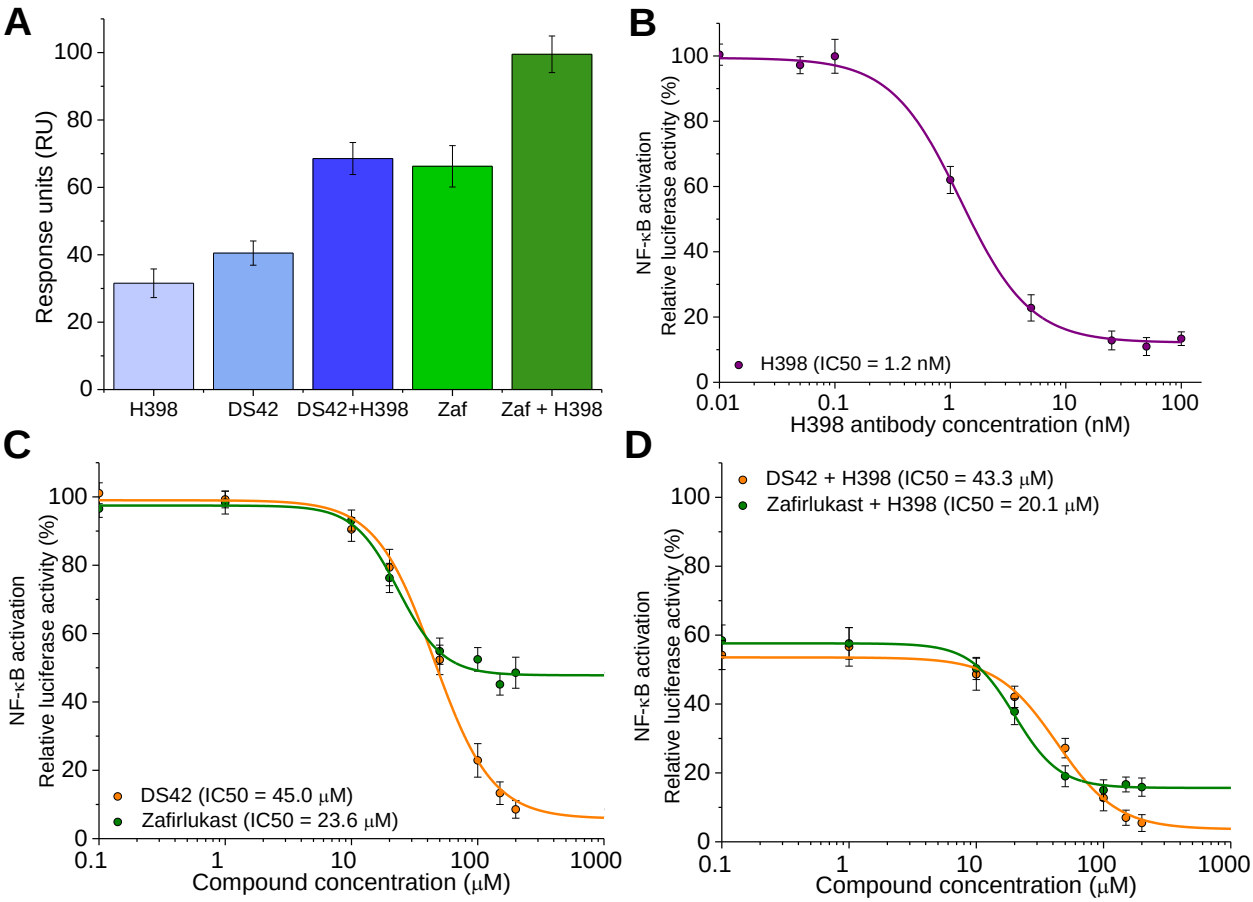

Fig. S9. Hit compounds do not compete with the H398 antibody in modulating TNFR1 signaling. (**A**) Noncompetitive binding assay using the H398 antibody (1 nM) and compounds (DS42 or zafirlukast at 200 μM) to TNFR1 ECD was performed by SPR. Data are means ± SD of three independent experiments. (**B**) NF-κB activation in HEK293 cells treated with LTα and increasing concentration of H398 antibody. Data are means ± SD of three independent experiments. (**C** and **D**) NF-κB activation in HEK293 cells treated with LTα and increasing concentration of compounds (DS42 and zafirlukast) in the absence (C) and presence of H398 antibody (1 nM) (D). Data are means ± SD of three independent experiments.

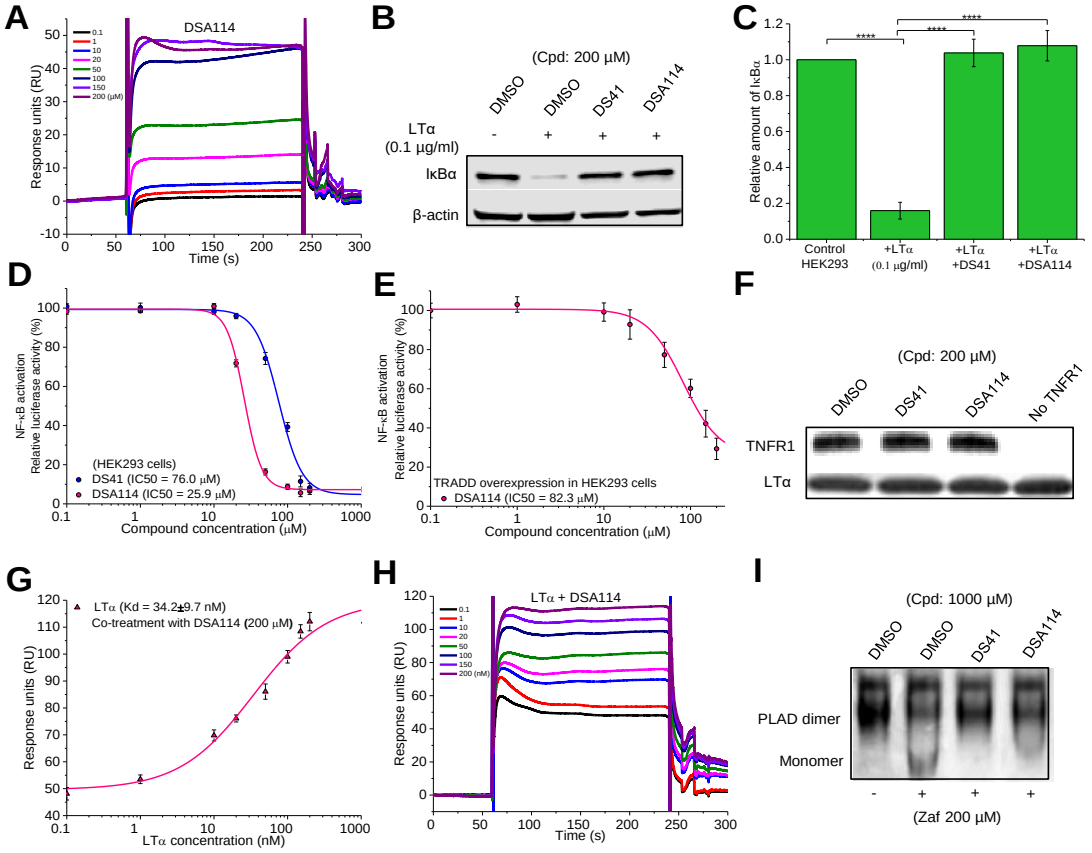

Fig. S10. DSA114, an analog of DS41, shows improved potency and specificity by acting through the same noncompetitive inhibition mechanism. (**A**) Surface plasmon resonance (SPR) raw curves for the binding of DSA114 to TNFR1 ECD. Binding curves are representative of three independent experiments. (**B** and **C**) Western blot analysis of IκBα abundance in lysates of HEK293 cells treated with LTα and the hit compound (DS41) and its analog (DSA114) at 200 μM. Western blots (B) are representative of three independent experiments. Quantified band intensity values (C) are means ± SD from all experiments. ****$P < 0.0001$ compared to control by two-tailed unpaired *t* test. (**D**) NF-κB activation in HEK293 cells treated with LTα and increasing concentration of hit compound (DS41) or its analog (DSA114) to test the improvements in the potency of the analog. Data are means ± SD of three independent experiments. (**E**) TRADD-induced NF-κB activation in HEK293 cells treated with increasing concentrations of DSA114. Data are means ± SD of three independent experiments. (**F**) Co-immunoprecipitation of TNFR1 and its ligand LTα from cells treated with DMSO vehicle, DS41 and DSA114 at a saturation dose of 200 μM. Equal amount of LTα is shown as pull-down controls. Western blots are representative of three independent experiments. (**G**) Dose-dependent binding of LTα in the presence of DSA114 at a saturated dose of 200 μM. Data are means ± SD of three independent experiments. (**H**) SPR raw curves of the dose-dependent binding of LTα to TNFR1 ECD in the presence of DSA114 (200 μM). Binding curves are representative of three independent experiments. (**I**) Native gel characterization of soluble TNFR1 PLAD from cells cotreated with DS41 or DSA114 (1000 μM) and zafirlukast (200 μM). Gels are representative of three independent experiments.

Table S1. Functional characterization of DS41 and its analogs. NF-κB activation in HEK293 cells treated with LTα and lead compound (DS41) or its analogs in a dose-dependent manner to characterize their functional potency.

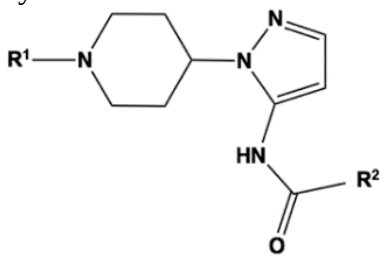

Cpd	R^1	R^2	NF-κB IC_{50} (μM)	NF-κB % inhibition	DIVERSet Cpd ID
1 (lead)	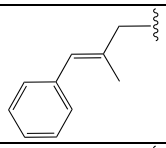	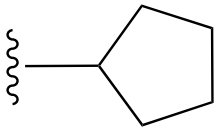	76.0	91.8%	19298144 (DS41)
2	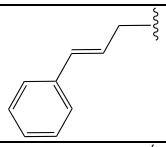	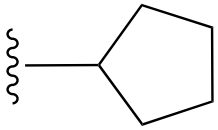	112.0	47.9%	55283788 (DSA103)
3	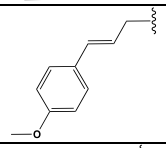	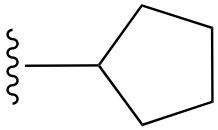	18.8	50.5%	75039431 (DSA104)
4	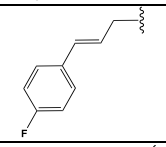	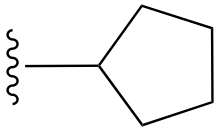	9.23	50.6%	50757273 (DSA105)
5	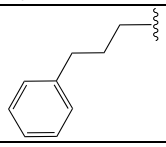	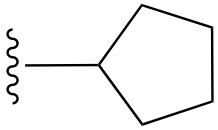	45.2	51.3%	74382948 (DSA106)
6	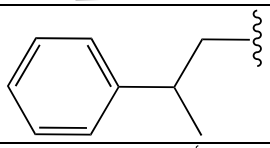	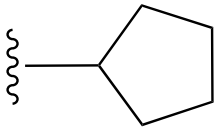	>200	0%	48067447 (DSA109)
7	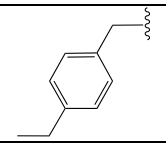	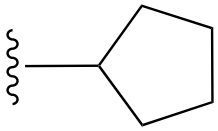	77.7	59.2%	38690331 (DSA108)
8	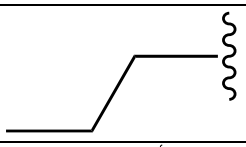	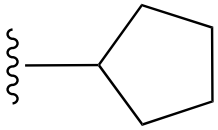	10.1	35.6%	84403474 (DSA102)
9	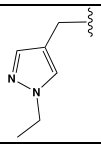	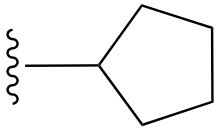	156.3	20.5%	33398307 (DSA110)

10	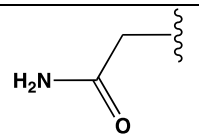	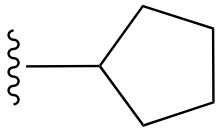	35.5	18.9%	95764424 (DSA117)
11	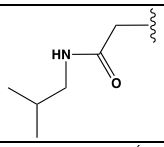	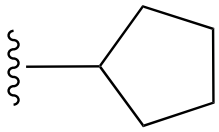	>200	0%	95807637 (DSA118)
12	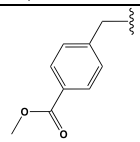	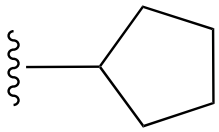	153.0	56.7%	92297604 (DSA119)
13	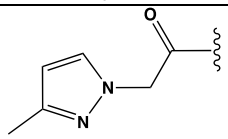	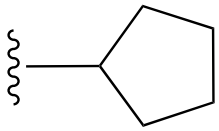	>200	0%	17903419 (DSA120)
14	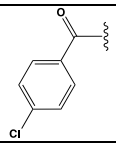	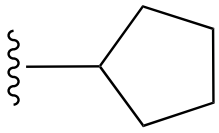	>200	0%	25121369 (DSA121)
15	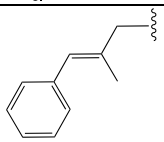	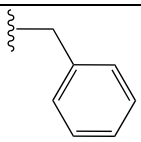	77.3	95.5%	52016291 (DSA111)
16	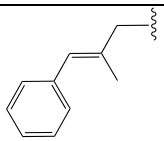	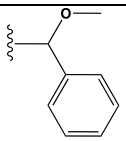	115.0	85.7%	74438793 (DSA112)
17	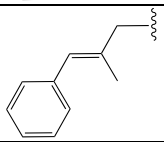	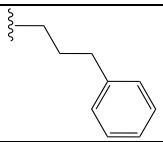	51.3	90.8%	41340052 (DSA113)
18	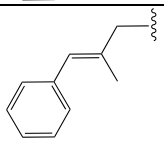	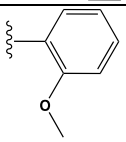	25.9	93.5%	16888972 (DSA114)
19	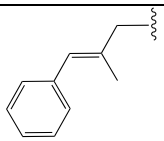	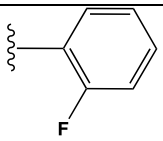	29.7	94.3%	59182823 (DSA115)
20	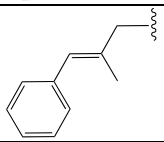	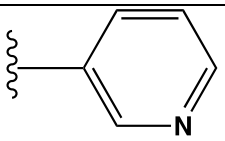	>200	0%	72564798 (DSA116)